IEEE Access
Multidisciplinary | Rapid Review | Open Access Journal

Received February 7, 2020, accepted February 14, 2020, date of publication February 19, 2020, date of current version February 28, 2020.

Digital Object Identifier 10.1109/ACCESS.2020.2975009

Design and Simulation of an Intelligent Current Monitoring System for Urban Rail Transit

CHENG YAO[1], QINGLEI ZHAO[2], ZELONG MA[2], WEI ZHOU[3], AND TONG YAO[3]

[1]University of Chinese Academy of Science, Beijing 100039, China
[2]Changchun Institute of Optics, Fine Mechanics and Physics, Chinese Academy of Sciences, Changchun 130033, China
[3]Xi'an Institute of Optics and Precision Mechanics, Chinese Academy of Sciences, Xi'an 710119, China

Corresponding author: Qinglei Zhao (zhaoql_ciomp@163.com)

This work was supported by the National Natural Science Foundation of China under Grant 11873046.

ABSTRACT Many urban rail transit (URT) systems adopt the DC traction power supply system. Because of the impedance and incomplete ground insulation of the running track, it is inevitable for a part of the traction current to flow into the ground from the track, creating the stray current. This type of current causes great safety hazards to the metal structures in and near the URT system. Considering the power supply mode of the URT, this paper explores the different resistances in each power supply section under unilateral power supply and bilateral power supply. Then, the defects of the current discharge method were identified in the context of stray current protection. To solve these defects, the backpropagation neural network (BPNN) was adopted to build a discharge flow prediction model. On this basis, an intelligent current monitoring system was established for the URT. Finally, the authors simulated the impact of each factor on stray current, and verified the reliability and stability of the proposed monitoring system. Compared with predicted values and the actual values, the prediction agrees with the actual data very well.

INDEX TERMS Urban rail transit (URT), backpropagation neural network (BPNN), stray current, current monitoring system.

I. INTRODUCTION

With the boom in urban rail transit (URT), the stability and safety of the URT system have become a major concern. In the URT, the train cannot operate safely and efficiently without a robust current system.

The rated voltage of traction power supply in the URT falls on multiple levels in the traditional range of DC 500-3,000V. During train operations, the traction current flows to the train via the catenary, and returns through the running track to the negative pole of the rectifier at the traction substation. Because of the impedance and incomplete ground insulation of the running track, it is inevitable for a part of the traction current to flow into the ground from the running track, and then back to the track and the substation. This part of current is called the stray current [1].

The stray current poses many threats to the URT, such as eroding the metal structures in and near the system. Calculations show that a stray current of 1A can erode 9.1kg metal within a year. The normal operation of the URT generates a large volume of stray current. It only takes a few years before the buried metal structures falling into disrepair, owing to the corrosion by the stray current.

The running track of the URT is often interlaced with underground municipal pipelines, ranging from gas pipeline, water supply pipeline to communication pipeline, which makes matters worse. To protect the URT operations and other underground facilities, it is imperative to identify the distribution law of stray current in the URT, and formulate effective measures to monitor the stray current.

In the light of the above, this paper attempts to design an intelligent monitoring system for the stray current in the URT. Firstly, the different resistances in each power supply section were examined under two modes of traction power supply. Next, the authors identified the defects of the current discharge method for stray current protection, and then built a discharge flow prediction model based on the backpropagation neural network (BPNN). On this basis, an intelligent current monitoring system was established for the URT, and verified through example analysis.

II. LITERATURE REVIEW

Many scholars have attempted to control the current in the URT. For instance, Shen and Jiang [2] examined the basic

The associate editor coordinating the review of this manuscript and approving it for publication was Dalin Zhang.

components and key technical parameters of the current monitoring system for URT trains. Focusing on the URT trains, Darong *et al.* [3] differentiated between the front and rear tractions of the electric drive system, through analysis on rectification, inversion, modulation and demodulation. Li *et al.* [4] divided the current monitoring system of the URT into several subsystems, and determined the basic elements of that system.

The stray current is the focus of the current monitoring system for the URT. Chen *et al.* [5] treated the distribution law of stray current as a complex current field problem, and held that the stray current distribution is affected by the design size of the URT system and the location of the train. Sheridan *et al.* [6] highlighted the complexity of the traction power supply system in the URT, as multiple traction stations need to supply power to multiple trains at the same time. Under the unilateral power supply mode, Jia *et al.* [7] built an analytical model of stray current distribution in the track-earth return system, using the following hypotheses: the catenary does not produce stray current onto the earth, and the positive pole of the traction substation at the receiving end of the train is not coupled with the earth. To reduce the total traction power and track potential, Chen *et al.* adjusted the time of each substation by the genetic algorithm (GA) to prevent the simultaneous starting and braking of multiple trains [8]–[10].

Currently, the URT parameters are measured either online or offline [11]–[13]. Wang *et al.* [14] proposed the field test method after analyzing the impacts of track-earth transition resistance, track potential and longitudinal track resistance on the return system. Liu *et al.* [15] put forward an approach to test the track-earth transition resistance under AC power supply, but the test approach faces large errors. Drawing on Newton's iteration, Daude *et al.* [16] developed an online measurement method for track-earth transition resistance. Using first-order differential equation, Haidar *et al.* [17] solved the continuous model of the return system with DC traction power supply, and discussed about the ways to test the track-earth transition resistance and track resistance.

In the URT, the stray current is mainly generated as the current returns to the DC traction power supply via the track. The monitoring and prevention of stray current require the synergy between various disciplines. Some scholars have investigated the harms of stray current and developed various countermeasures that integrate prevention, discharge and interception. For example, Zhou and Xing [18] explored the stray current monitoring system based on Foundation Fieldbus (FF), and detailed the architecture, software and hardware of the system. Di [19] compared the merits and defects of centralized and decentralized strategies of current monitoring, developed a distributed current monitoring strategy, and verified its effectiveness through field test. Johnston [20] proposed the array electrode method to measure the potential distribution at the interface of concrete reinforcement and at different depths. Cai *et al.* [21] probed into the monitoring methods of stray current on corroded long-distance pipelines. Zhao *et al.* [22] tackled the IR-drop error through polarization potential test, theoretically derived the double reference electrode method to eliminate the IR-drop, and experimentally proved that the method can eliminate the IR-drop, which exists in the stray current monitoring of the URT.

III. STRAY CURRENT MODEL OF THE URT

The URT has a very complex DC traction power supply system, which mainly consists of a regional substation (or grid-connected step-down substation), an external power supply system, a special electrical system (including a DC traction substation and a step-down substation), and a track area. The architecture of the DC traction power supply system is shown in Figure 1 below.

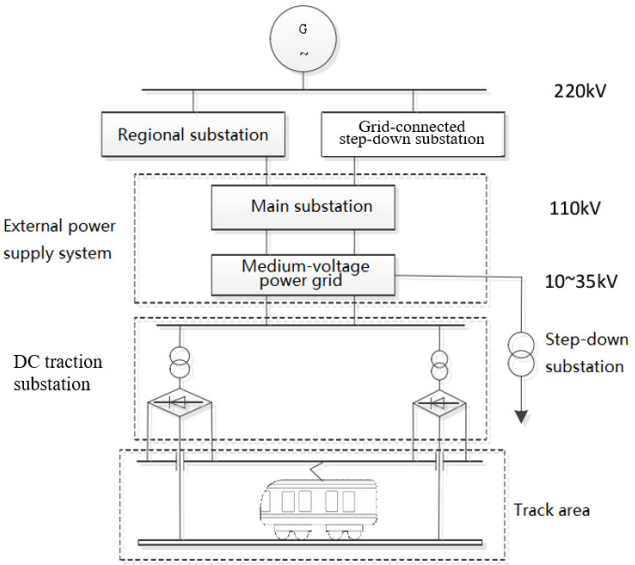

FIGURE 1. The architecture of the DC traction power supply system of the URT.

Before setting up a current monitoring system of the URT, it is necessary to clarify the operation mode of the traction power supply system. In general, there are two types of operation modes for the said system, namely, unilateral power supply and bilateral power supply. For a train running in a power supply section, it is powered only by a nearby traction substation under the former operation mode, and powered by two front traction substations nearby under the latter operation mode.

In the DC traction power supply system of urban rail transit, the traction substation is fed to the catenary, and the current flows back to the negative pole of the traction substation through the running rail after passing through the electric locomotive. In the process of rail return, part of the current flows into the underground through the track bed, and two corrosion cells will be formed underground. The metal in these two areas will be corroded by electrolysis. In the process of corrosion, the chemical reaction process is also different according to the surrounding acid and alkali environment. Hydrogen evolution corrosion occurs when metals

are corroded in acid environment, and oxygen absorption corrosion occurs when metals are corroded in alkaline environment.

On this basis, the following constrains were put forward for the stray current distribution under the mode of unilateral power supply:

(1) The track has a uniform longitudinal resistance;

(2) The track-earth transition resistance is uniform;

(3) The earth has a uniform longitudinal resistance, which is infinitely close to zero;

(4) The system impedance of traction substation(s), feeder, and catenary is negligible.

Under the above constraints, the track-earth resistance under the mode of unilateral power supply was modelled as Figure 2, where R_g is the track-earth resistance, R is the longitudinal resistance of the track, and I is the traction current of the train.

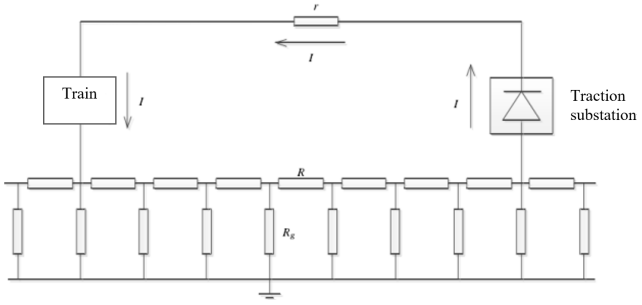

FIGURE 2. The rail-earth resistance under the mode of unilateral power supply.

Note: R_g represents track-earth transition resistance, R represents rail longitudinal resistance, I represents traction current of electric locomotive.

The current flow path of track-earth resistance is shown in Figure 3, where x is the distance to the traction substation, and $i(x)$ is the track current at x.

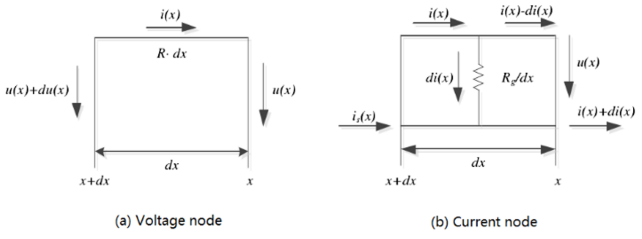

FIGURE 3. The current flow path of track-earth resistance.

According to Kirchhoff's voltage law (KVL), the following equation can be derived from Figure 3(a):

$$i(x) \cdot R \cdot dx + u(x) - [u(x) + du(x)] = 0 \tag{1}$$

where $i(x)$ represents current, R represents the longitudinal resistance of the rail, $u(x)$ represents rail potential at position x.

TABLE 1. The value range of each parameter.

Name	Symbol	Value range
Longitudinal resistance of track	R_s	0-0.2
Track-earth transition resistance	R_d	0-200
Longitudinal resistance of earth	R_l	0.001-1
Earth-buried metal transition resistance	R_t	0-200
Longitudinal resistance of buried metal	R_b	0.001-1
Length of power supply section	D	2.5-5
Traction current of the train	I	600-4000

Equation (1) can be simplified as:

$$du(x) = i(x) \cdot R \cdot dx \tag{2}$$

Similarly, the following equation can be derived from Figure 3(b):

$$u(x) = di(x) \cdot \frac{R_g}{dx} \tag{3}$$

R_g represents rail-ground transition resistance.

Solving (3), we have:

$$di(x) = \frac{u(x)}{R_g} \cdot dx \tag{4}$$

According to (2), we have:

$$\frac{d^2u(x)}{du^2} = \frac{di(x)}{dx} \cdot R \tag{5}$$

Substituting (4) into (5), we have:

$$\frac{d^2u(x)}{du^2} - \frac{R}{R_g} \cdot u(x) = 0 \tag{6}$$

Assuming that $\alpha^2 = \frac{R}{R_g}$, (6) can be transformed as:

$$\frac{d^2u(x)}{du^2} - \alpha^2 \cdot u(x) = 0 \tag{7}$$

The general solution of (7) can be expressed as:

$$u(x) = \varphi ch\alpha x + \omega sh\alpha x \tag{8}$$

where, φ and ω are indefinite coefficients.

Taking the derivatives of (8) on both sides, we have:

$$\frac{du(x)}{dx} = \alpha(\varphi ch\alpha x + \omega sh\alpha x) \tag{9}$$

Substituting (9) into (2), we have:

$$i(x) = \frac{1}{\sqrt{RR_g}}(\varphi ch\alpha x + \omega sh\alpha x) \tag{10}$$

According to (10), the indefinite coefficients φ and ω can be solved as:

$$\begin{cases} \varphi = -\sqrt{RR_g} \cdot I \cdot th\dfrac{\alpha}{2}L \\ \omega = \sqrt{RR_g} \cdot I \end{cases} \tag{11}$$

In the URT, the stray current distribution is affected by many environmental factors. To disclose the basic law of stray current distribution, the stray current model was applied for the URT simulation. According to the value ranges in Table 1,

the model parameters were configured as follows before the simulation: $R_s = 0.02$, $R_d = 20$, $R_l = 0.015$, $R_t = 5$, $R_b = 0.015$, $D = 3.5$ and $I = 3,000$.

First, the URT was simulated under the two power supply modes, and the distributions of track potential and stray current were observed. The distance between the train and the traction substation was 1km and 2km under the unilateral power supply mode and the bilateral power supply mode, respectively. According to the simulation results, the effects of power supply modes on track potential and stray current are presented in Figures 4 and 5, respectively.

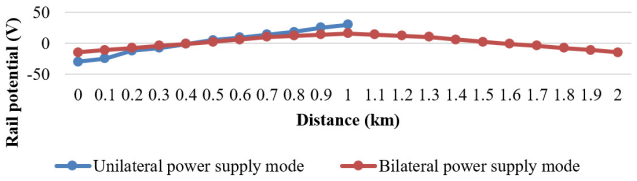

FIGURE 4. The effects of power supply modes on track potential.

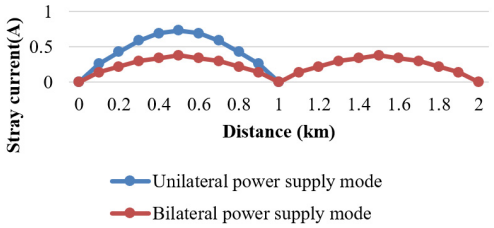

FIGURE 5. The effects of power supply modes on stray current.

The simulation results show that the distributions of track potential and stray current between the train and the traction substation were similar between the two power supply modes. The track potential decreased monotonically from the positive maximum at the train towards the negative maximum at the traction substation, passing through a point of zero track potential. The stray current distribution takes the shape of a parabolic curve between the train and the substation.

The tack potential and stray current were higher under the bilateral power supply mode than under the unilateral power supply mode. This is because the train is powered by the traction substations on both sides under the former mode and by only one substation under the latter mode. Since the distributions of track potential and stray current follow the same trend under the two modes, the unilateral power supply mode was adopted to analyze the influence of other factors in subsequent simulations.

IV. BPNN-BASED URT CURRENT MONITORING

In the URT, several parameters are the key targets of stray current monitoring, including longitudinal track resistance, track-earth transition resistance and track potential. The weights of these parameters can be determined by their sensitivity to stray current corrosion.

In the URT current monitoring system, there is no exact relationship between the discharge flow and polarization potential. The stray current flowing from track to earth can be captured by the current discharge protection method.

To enhance the discharge protection effect, it is necessary to build an artificial neural network (ANN)-based model that predicts the discharge flow, according to the polarization potentials of multiple monitoring points.

Here, the discharge flow is modelled based on the BPNN [23], which is good at solving nonlinear problems with no exact relationship between the input and output. The BPNNs generally have three or more layers, each of which has multiple neurons.

In the URT, the current discharge mainly occurs under the polarization potential of the metal structure. For each power supply section, a total of 16 reference electrodes were deployed at different positions to capture the polarization potential of every metal structure.

According to the multi-point evaluation principle of discharge protection, the polarization potential should be evaluated at five points at the least. In this paper, the number of evaluation points is set to 6, and these points have different impacts on discharge flow. The mean value of the forward propagation of the 6 monitoring points was taken as the input of the BPNN, and the proportion factor μ of the discharge flow was taken as the output. Thus, the structure of the BPNN-based discharge prediction model is presented in Figure 6.

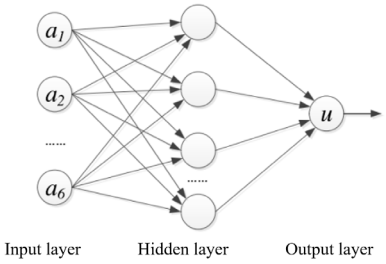

FIGURE 6. The BPNN-based discharge prediction model.

The hidden layer is the core of the entire BPNN. The number of neurons on this layer directly bears on the network performance. The number of hidden layer neurons n_h can be empirically calculated by:

$$n_h = \sqrt{c + d} + t \tag{12}$$

where, c is the number of input layer neurons; d is the number of output layer neurons; t is a constant in [1], [10].

Through calculation, the number of neurons on the input layer, hidden layer and output layer were set to 6, 10 and 1, respectively.

The BPNN can memorize the patterns of the problem through data training. Hence, the training data must cover all the characteristic patterns of the problem. In our model, the polarization potentials measured at the six monitoring points

are taken as the inputs of the sample data, and the discharge factor was taken as the output.

The sample data were imported to the BPNN-based model, with the error of 0.00001 as the training target. After 29 iterations, the error of the BPNN was 0.00008961, which achieves the training target.

To verify its performance, the BPNN-based model was tested by the sample data in Table 2. The predicted values and the actual values are compared in Figure 7. The comparison shows that the prediction agrees well with the actual data.

TABLE 2. Test sample data.

No.	a_1	a_2	a_3	a_4	a_5	a_6	μ
1	0.126	0.127	0.031	0.045	0,028	0.017	0.627
2	0.286	0.289	0.052	0.092	0.024	0.021	0.905
3	0.575	0.581	0.065	0.084	0.033	0.052	0.880
4	0.723	0.698	0.081	0.055	0.028	0.056	0.755
5	0.656	0.720	0.035	0.065	0.033	0.066	0.825
6	0.325	0.337	0.023	0.043	0.022	0.125	0.765
7	0.118	0.121	0.062	0.037	0.092	0.037	0.900
8	0.066	0.083	0.036	0.072	0.105	0.055	0.255
9	0.072	0.075	0.042	0.068	0.097	0.062	0.590
10	0.122	0.128	0.065	0.096	0.098	0.115	0.980

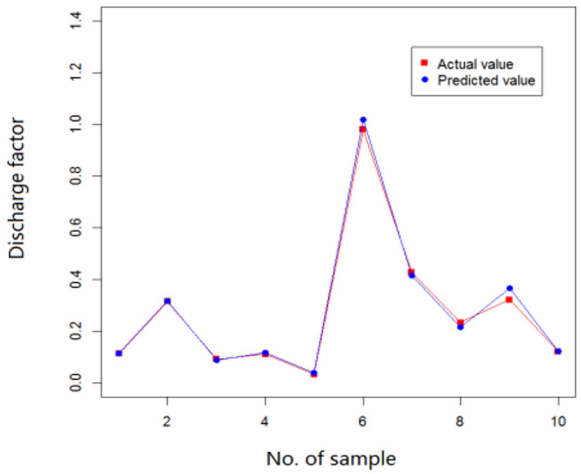

FIGURE 7. Comparison between predicted values and actual values.

As shown in Figure 7 and Table 2, the predicted values of the BPNN-based model only deviated from the actual values of the ten groups of sample data by 0.05, indicating that our model can effectively predict the discharge flow after training.

V. CONCLUSION

This paper introduces the architecture of the transit power supply system in the URT, analyzes the formation of stray current in URT operations, and simulates the degrees of impacts from various factors on the stray current. On this basis, the authors established a current monitoring system for the URT. First, the measurement method for monitoring parameters was discussed in details. Next, the defects of current discharge method were analyzed, in the context of stray current protection. To solve the defects, a stray current monitoring system was developed based on the BPNN. Finally, the effectiveness of the proposed system was proved through data verification. Therefore, the analysis of the distribution law of the current and the adoption of effective current monitoring methods and protective measures will have positive significance for the design, construction and safe and reliable operation of urban rail transit in the future.

REFERENCES

[1] L. Bertolini, M. Carsana, and P. Pedeferri, "Corrosion behaviour of steel in concrete in the presence of stray current," *Corrosion Sci.*, vol. 49, no. 3, pp. 1056–1068, Mar. 2007.

[2] X. J. Shen and X. C. Jiang, "Development of online monitoring system for 1500 v ethylene–propylene–rubber DC feeder cable of shanghai urban rail transit," *IET Gener., Transmiss. Distrib.*, vol. 5, no. 7, pp. 720–730, 2011.

[3] H. Darong, K. Lanyan, C. Xiaoyan, Z. Ling, and M. Bo, "Fault diagnosis for the motor drive system of urban transit based on improved hidden Markov model," *Microelectron. Rel.*, vol. 82, pp. 179–189, Mar. 2018.

[4] X. Li, X. N. Zhu, and G. Q. Cai, "Research on system integration alliance of urban rail transit safety monitoring," *J. Converg. Inf. Technol.*, vol. 5, no. 7, pp. 36–41, Sep. 2010.

[5] Z. G. Chen, C. K. Qin, Y. J. Zhang, and J. X. Tang, "Research of impact of stray current from urban rail transit system on buried gas pipeline," *Adv. Mater. Res.*, vols. 239–242, pp. 1219–1222, May 2011.

[6] R. Sheridan, J. Roche, S. E. Lofland, and P. R. vonLockette, "Numerical simulation and experimental validation of the large deformation bending and folding behavior of magneto-active elastomer composites," *Smart Mater. Struct.*, vol. 23, no. 9, Aug. 2014, Art. no. 094004.

[7] X. F. Jia, Y. F. Ma, J. Huang, and C. Y. Zhao, "Research on earth-return current and grounding grid potential rise in traction substation," *Power Syst. Protection Control*, vol. 40, no. 10, pp. 116–119, 2012.

[8] J.-F. Chen, R.-L. Lin, and Y.-C. Liu, "Optimization of an MRT train schedule: Reducing maximum traction power by using genetic algorithms," *IEEE Trans. Power Syst.*, vol. 20, no. 3, pp. 1366–1372, Aug. 2005.

[9] H. Özdemir, R. Sever, and Ö. Polat, "GA-based optimization of SURF algorithm and realization based on vivado-HLS," *Traitement du Signal*, vol. 36, no. 5, pp. 377–382, Nov. 2019.

[10] B. Zheng and Y. Zhong, "Study on the impacts of urban network evolution on urban wind and heat environment based on improved genetic algorithm," *Ingénierie des Systèmes D'information*, vol. 23, no. 5, pp. 105–119, Oct. 2018.

[11] L. Dong, J. Wu, and W. Wang, "A safe evacuation mode for ultradeep underground space in urban rail transit stations," *J. Européen des Systèmes Automatisés*, vol. 52, no. 4, pp. 377–385, Oct. 2019.

[12] G. Sun, S. Bin, and C.-C. Chen, "Reliability analysis of complex brain networks based on chaotic time series," *Microelectron. Rel.*, vol. 99, pp. 295–301, Aug. 2019.

[13] J.-C. Schauer, S. Hong, and J. Winter, "Electrical measurements in dusty plasmas as a detection method for the early phase of particle formation," *Plasma Sources Sci. Technol.*, vol. 13, no. 4, pp. 636–645, Oct. 2004.

[14] C. Wang, W. Li, Y. Wang, S. Xu, and M. Fan, "Stray current distributing model in the subway system: A review and outlook," *Int. J. Electrochem. Sci.*, vol. 13, pp. 1700–1727, Feb. 2018.

[15] K. Liu, S. Liang, H. Shu, X. Luo, and W. Wu, "Influence of transition resistance on transient power converse in UHV AC/DC hybrid power system," *High Voltage Eng.*, vol. 41, no. 4, pp. 1257–1261, 2015.

[16] F. Daude, I. Mary, and P. Comte, "Self-adaptive Newton-based iteration strategy for the LES of turbulent multi-scale flows," *Comput. Fluids*, vol. 100, pp. 278–290, Sep. 2014.

[17] A. M. A. Haidar, A. Mohamed, and F. Milano, "A computational intelligence-based suite for vulnerability assessment of electrical power systems," *Simul. Model. Pract. Theory*, vol. 18, no. 5, pp. 533–546, May 2010.

[18] Z. Q. Jiang and R. H. Li, "Intelligent aquaculture monitoring system based on fieldbus," *Appl. Mech. Mater.*, vols. 263–266, pp. 427–430, Dec. 2012.

[19] R. G. Di, "Research on the monitoring system for stray current in urban rail transit system," *Adv. Mater. Res.*, vols. 433–440, pp. 1811–1814, Jan. 2012.
[20] B. M. Johnston, "Using a sensitivity study to facilitate the design of a multi-electrode array to measure six cardiac conductivity values," *Math. Biosci.*, vol. 244, no. 1, pp. 40–46, Jul. 2013.
[21] L. H. Cai, W. Li, and H. F. Fang, "Monitoring method of stray current in coal mine on optical fiber sensing technique," *Appl. Mech. Mater.*, vol. 43, pp. 457–462, Dec. 2010.
[22] S. Zhao, I. Ahmed, V. Betz, A. Lotfi, and O. Trescases, "Frequency-domain power delivery network self-characterization in FPGAs for improved system reliability," *IEEE Trans. Ind. Electron.*, vol. 65, no. 11, pp. 8915–8924, Nov. 2018.
[23] G. Sun and S. Bin, "A new opinion leaders detecting algorithm in multi-relationship online social networks," *Multimedia Tools Appl.*, vol. 77, no. 4, pp. 4295–4307, Nov. 2017.

CHENG YAO was born in Changchun, Jilin, China, in 1991. He received the B.E. degree from the Changchun University of Science and Technology, in 2013, and the master's degree in mechanical engineering from the Changchun Institute of Optics, Fine Mechanics and Physics, CAS, and the University of Chinese Academy of Sciences, in 2016. He is currently pursuing the Ph.D. degree with the Xi'an Institute of Optics and Precision Mechanics, CAS, and the University of Chinese Academy of Sciences. His main research interests include electronic control, power supply systems, and 3D Reconstruction.

QINGLEI ZHAO was born in Daqing, Heilongjiang, China, in 1982. He received the Ph.D. from the University of Chinese Academy of Sciences, China. He is currently working with the Changchun Institute of Optics, Fine Mechanics and Physics. He is mainly involved in the research of embedded system design and automatic control.

ZELONG MA was born in Changchun, Jilin, China, in 1985. He received the Ph.D. degree from the University of Chinese Academy of Sciences, in 2018. He is currently an Assistant Researcher with the Changchun Institute of Optics, Fine Mechanics and Physics, Chinese Academy of Sciences. His main research directions are servo control and electronic circuits.

WEI ZHOU was born in Changsha, Hunan, China, in 1992. He received the B.E. degree in electronic and information engineering from Xidian University, in 2013. He is currently pursuing the Ph.D. degree with the Xi'an Institute of Optics and Precision Mechanics, CAS, and the University of Chinese Academy of Sciences. He is also visiting Fraunhofer IGD and TU Darmstadt. His main research interests include 3D recognition, 3D feature matching, and other point-cloud-based researches.

TONG YAO was born in Xianyang, Xi'an, China, in 1992. She received the B.S. degree in mathematics and applied mathematics from Hunan University, in 2013. She is currently pursuing the Ph.D. degree with the Xi'an Institute of Optics and Precision Mechanics, CAS, and the University of Chinese Academy of Science. Her main research interest is video semantic analysis.